Three-Dimensional Slope Stability Model Using Finite Element Stress Analysis

Gilson Gitirana Jr.[1], Marcos A. Santos[2], and Murray D. Fredlund[3]

[1]Professor, School of Civil Engineering, Federal University of Goias, Goiania, GO, Brazil; gilsongj@eec.ufg.br
[2]Ph.D. student, Dep. of Civil and Environmental Engn., University of Brasilia, Brasilia, DF, Brazil; marcosairess@gmail.com
[3]President, SoilVision Systems Ltd., 202-640 Broadway Ave., Saskatoon, SK, Canada S7N 1A9; murray@soilvision.com

ABSTRACT: A practical three-dimensional slope stability approach is presented. Simple finite element stress and seepage analyses are employed in order to computer factors of safety. Benchmark problems are presented in order to verify the accuracy of the proposed method. Close agreement is observed when comparing the results obtained herein and those from the literature.

INTRODUCTION

Most slope stability problems are three-dimensional in nature. Few are the situation where a two-dimensional plane strain condition truly represents the field condition. Several field conditions can be better represented by three-dimensional models, such as excavation fronts, slope corners, dam shoulders, to name only a few geotechnical problems. Numerous advances in three-dimensional geotechnical analysis have been achieved in the last few decades, mostly due to the increase in computational power.

This paper presents how three-dimensional slope stability analyses can be undertaken using simple finite element stress and seepage analysis. Two benchmark problems are presented in order to demonstrate the accuracy of the method of analysis.

LITERATURE REVIEW

The methods of three-dimensional analysis of slopes are usually extensions of conventional two-dimensional approaches. Variational calculus, for instance, has been extended to three-dimensional conditions by Leshchinsky et al. (1985) and Leshchinsky and Baker (1986). Leshchinsky and Huang (1992) further extended their original work, but the method was limited to problems with symmetric geometry.

Michalowski (1989) presented a three-dimensional solution based on the upper-

bound theorem. The solution was limited to homogeneous slopes. More recently, Farzaneh and Askari (2003) have extended the work by Michalowski (1989) to non homogeneous slopes. Chen et al (2001a, 2001b) have also presented an upper-bound solution for three-dimensional slope stability.

Lam and Fredlund (1993) have presented an extension of the GLE limit equilibrium method to three-dimensional conditions. The method is particularly interesting considering that the limit equilibrium is widely accepted in geotechnical engineering practice.

Other modeling approaches have been presented by numerous researchers in the last few years. The upper and lower-bound theorems have been applied along with the finite element method, in order to produce stress and strain fields (Lyamin and Sloan, 2002a and 2002b).

From the point of view of practicing geotechnical engineers, it becomes difficult to determine what three-dimensional method of slope stability analysis is the more adequate. A sound theoretical basis, a generalized approach that is capable of handling field conditions, and simplicity, are some of the requirements of a handy slope stability method. It appears that if a practical three-dimensional finite element tool for stress and seepage analysis is available, it becomes convenient to extend the two-dimensional enhanced method to three-dimensional conditions. Such method could be considered a practical tool for routine analyses.

THEORY

The factor of safety is usually defined as the ratio by which the shear strength must be reduced in order to bring the soil mass to a state of limit equilibrium. For a three-dimensional slip surface, the factor of safety may be computed by taking the total resisting shear force divided by the total shear force:

$$F_s = R/S = \int_A \tau_f \, dA \Big/ \int_A \tau_a \, dA \qquad (1)$$

where: R is the total resisting shear force; S is the total shear force; τ_f is the shear strength; τ_a is the shear stress; and A is the slip surface area.

The resisting and shearing stresses acting along a three dimensional slip surface must be determined. The state of stress and pore-water pressure at any point in the soil volume may be determined using the finite element method. Therefore, the method presented herein is an extension of the enhanced method to three-dimensional conditions. The computation of the factor of safety can be summarized as follows:

a) The distribution of stresses and pore-water pressures are determined using the finite element method. Appropriate boundary conditions, constitutive models, and constitutive parameters must be adopted;
b) The normal and shear stresses are computed for a grid of points located at the base of the slip surface. The normal stress depends on the position along the slip surface. The shear stress depends not only on the position at the slip surface but also on the direction of slippage projected on the horizontal plane;

c) Integration of the acting and resisting stresses is performed along the slip surface area.

Spherical and ellipsoidal slip surface shapes have been implemented and tested herein. The shape and position of a spherical slip surface are defined as follows:

$$z = z_{0s} - \sqrt{r_s^2 - (x - x_{0s})^2 - (y - y_{0s})^2} \tag{2}$$

where: x_{0s}, y_{0s}, and z_{0s} are the coordinates of the center of the sphere in the x, y, and z directions; and r_s is the radius of the slip surface. Only the bottom half of the sphere is taken by using the minus sign for the square root.

The shape and position of an ellipsoidal slip surface can be defined as follows:

$$z = z_{0e} - c\sqrt{1 - \frac{[(x - x_{0e})\cos\theta + (y - y_{0e})\sin\theta]^2}{a^2} - \frac{[(y - y_{0e})\cos\theta - (x - x_{0e})\sin\theta]^2}{b^2}} \tag{3}$$

where: x_{0e}, y_{0e}, and z_{0e} are the coordinates of the center of the ellipsoid; a, b, and c are the lengths of the semi-axes in the x, y, and z directions; and θ gives the orientation of the ellipsoid in the x-y plane, θ being 0 in the x-direction and increasing counter-clockwise.

The direction of a plane tangent to any point of the slip surface is defined by the angles its normal makes with x, y, and z. Such direction can be expressed in terms of the direction cosines:

$$a_{11} = \frac{\partial f/\partial x}{\|f\|};\ a_{21} = \frac{\partial f/\partial y}{\|f\|};\ a_{31} = \frac{\partial f/\partial z}{\|f\|} \tag{4}$$

where: f denotes the equation defining the geometric location of the slip surface (Eqs. 2 or 3) and $\|f\| = \sqrt{(\partial f/\partial x)^2 + (\partial f/\partial y)^2 + (\partial f/\partial z)^2}$. The first index "1" indicates the direction defined by the normal to the surface. The second indexes indicate the x, y, and z directions

For a spherical slip surface, the derivatives are as follows:

$$\partial f/\partial x = 2(x - x_{0s});\ \partial f/\partial y = 2(y - y_{0s});\ \partial f/\partial z = 2(z - z_{0s}) \tag{5}$$

For an ellipsoidal slip surface, the derivatives are as follows:

$$\partial f/\partial x = 2[(x - x_{0e})\cos\theta + (y - y_{0e})\sin\theta]\cos\theta/a^2 - 2[(y - y_{0e})\cos\theta - (x - x_{0e})\sin\theta]\sin\theta/b^2 \tag{6}$$

$$\partial f/\partial y = 2[(x - x_{0e})\cos\theta + (y - y_{0e})\sin\theta]\sin\theta/a^2 + 2[(y - y_{0e})\cos\theta - (x - x_{0e})\sin\theta]\cos\theta/b^2 \tag{7}$$

$$\partial f/\partial z = 2(z - z_{0e})/c^2 \tag{8}$$

The normal stress acting in a plane tangent to any point of the slip surface is given by the following equation:

$$\sigma_n = \sigma_x a_{11}^2 + \sigma_y a_{21}^2 + \sigma_z a_{31}^2 + 2\tau_{xy} a_{11} a_{21} + 2\tau_{yz} a_{21} a_{31} + 2\tau_{zx} a_{31} a_{11} \quad (9)$$

Given the computed σ_n, the shear strength can be calculated using the Mohr-Coulomb criterion for saturated/unsaturated soils:

$$\tau_f = c' + (\sigma_n - u_a) \tan \phi' + (u_a - u_w) \tan \phi^b \quad (10)$$

where: c' is the effective cohesion; u_a is the pore-air pressure; ϕ' the angle of internal friction; u_w is the pore-water pressure; and ϕ^b is the angle of friction with respect to changes in matric suction. Equation 10 reduces to the conventional Mohr-Coulomb criterion when the soil becomes saturated.

In order to compute the acting shear stress, the direction of slippage movement must be known. The direction of the slippage movement may be determined as part of the optimization technique used in the determination of the critical slip surface. The slippage direction may also be adopted. For instance, the slippage movement could be assumed to be given by the average slope face direction.

The projection of slippage direction in the horizontal plane is given by a unit vector with components in the x and y direction, b_1 and b_2. The third component, b_3, indicates the direction normal to the slip surface and is orthogonal to b_1 and b_2:

$$b_3 = (-a_{11} b_1 - a_{21} b_2) / a_{31} \quad (11)$$

The direction cosines that indicate the slippage direction are as follows:

$$a_{12} = b_1 \Big/ \sqrt{b_1^2 + b_2^2 + b_3^2} \; ; \; a_{22} = b_2 \Big/ \sqrt{b_1^2 + b_2^2 + b_3^2} \; ; \; a_{32} = b_3 \Big/ \sqrt{b_1^2 + b_2^2 + b_3^2} \quad (12)$$

Finally, the shear stress acting at any point and slippage direction at the base of the slip surface is given by the stress state and direction cosines, defined by Eqs. 4 and 12:

$$\tau_a = \sigma_x a_{11} a_{12} + \sigma_y a_{21} a_{22} + \sigma_z a_{31} a_{32} + \tau_{xy} (a_{11} a_{22} + a_{21} a_{12}) + \tau_{yz} (a_{21} a_{32} + a_{31} a_{22}) + \tau_{zx} (a_{31} a_{12} + a_{11} a_{32}) \quad (13)$$

Finite Element models usually employ procedures based on stresses that are computed at the integration points. Therefore, in order to compute the normal and shear stress at any point at the base of a given slip surface, the state of stress determined at the integration points must be used. If necessary, these stresses can be extrapolated to the nodes using simple mapping techniques.

The procedure presented above must be employed for each trial slip surface established during the optimization analysis. Several optimization techniques are available for the determination of the critical slip surface. This paper will not deal with these procedures. Instead, the computation of the factor of safety of three-dimensional slip surfaces with known shape and position is presented.

ANALYSIS OF BENCHMARK PROBLEMS

There are few numerical modeling tools available that are capable of performing three-dimensional analysis. Most of the available tools are not practical and efficient enough for routine use. The analyses presented herein were performed using the software SVOffice 2006 (SoilVision Systems Ltd., 2007). The formulation presented above was programmed using FlexPDE (PDE Solution Inc., 2007), a general purpose partial differential equation solver. For the benchmark analyses presented herein, problem setup time was less than 15 minutes. The computation work usually took less than 5 minutes on a Core 2 Duo processor running at 2 GHz, with 1 Gb or RAM.

Two benchmark problems have been selected for the verification of the three-dimensional slope stability analysis solution. The first problem corresponds to a simple and symmetric cohesive slope. The second problem corresponds to an asymmetric slope with friction and cohesion. Both problems have been frequently presented in the research literature for benchmark purposes.

Symmetric Cohesive Slope

Figure 1a presents the first benchmark problem. A spherical slip surface is employed. The simple geometry, boundary conditions and soil properties allowed for the development of analytical solutions. Baligh and Azzouz (1975) and Gens et al. (1988) present two different solutions. Hungr et al. (1989), Lam and Fredlund (1993) and Chen et al. (2001) have also analyzed this problem.

The parameters adopted herein for the stress analysis where as follows: a Young Modulus of 3500 kPa; Poisson's ratio that varied from 0.1 to 0.49; total cohesion of 0.1 kPa, friction angle equal to zero; pore-water pressure equal to zero; and unit weight of 1 kN/m^3.

Figure 1b presents the distribution of vertical stresses throughout the slope and at the base of the slip surface. The simple geometry and absence of external loads results in smooth contours for the distribution of stresses.

Table 1 presents the results of the analysis along with the factors of safety obtained by other researchers using different methods of analysis. It can observed that similar results where obtained when comparing the numbers provided by all authors. The factor of safety obtained previously ranges from 1.386 to 1.422. The GLE method (Lam and Fredlund, 1993) provided a factor of safety of 1.402 when using a relatively small number of columns, 540. The three-dimensional enhance method used herein provides factors of safety near 1.4. However, the results depend on the value of Poisson's ratio. Values of factor of safety as high as 1.438 were obtained when increasing Poisson's ratio near its maximum theoretical value of 0.5.

A variation of 0.05 in the factor of safety was obtained when subjecting the analysis to extreme variations in the number of nodes. The number of nodes was varied from approximately 5,000 to up to 300,000. The size of the problem domain could also affect the results if the boundaries are too close to the slip surface. Increasing of the problem size did not result in significant changes in the factor of safety (less than 2% of variation). Therefore, the original domain size, presented in Fig. 1, was deemed adequate.

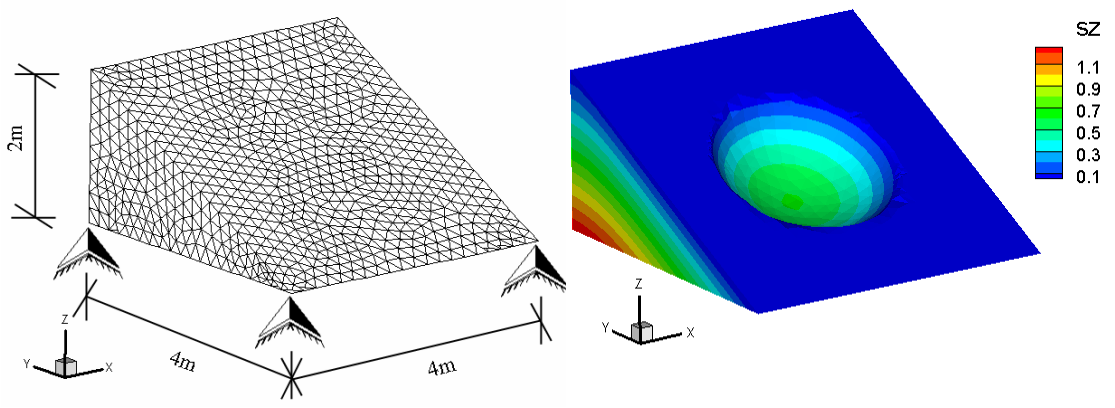

(a) (b)

FIG. 1. Benchmark problem 1 - homogeneous cohesive slope with spherical slip surface: (a) geometry and boundary conditions; and (b) vertical stresses.

Table 1. Benchmark problem 1: factors of safety obtained by other research and obtained in this study.

Reference	Method of analysis	F_s 3-D
Baligh and Azzouz (1975)	Analytical solution	1.402
Gens et. al. (1988)	Analytical solution	1.402
Hungr et. al. (1989)	Method of slices (Bishop's simplified)	1.422
Lam and Fredlund (1993), 540 columns	Method of slices (GLE)	1.402
Lam and Fredlund (1993), 1200 columns	Method of slices (GLE)	1.386
Chen et, al. (2001)	Upper bound theorem	1.422
This study	Poisson's ratio = 0.1	1.396
	Poisson's ratio = 0.2	1.401
	Poisson's ratio = 0.3	1.409
	Poisson's ratio = 0.4	1.422
	Poisson's ratio = 0.49	1.438

Non-symmetrical slope with friction and cohesion

Leshchinsky et al. (1985) have proposed an analytical solution for three-dimensional slope stability problems using the logarithmic spiral. One of the examples presented by Leshchinsky et al. (1985) is re-analyzed herein, using a spherical slip surface approximation. The same problem was also analyzed by Hungr et al. (1989) and Stianson (2006), using different approaches.

The parameters adopted herein for the stress analysis where as follows: a Young Modulus of 3500 kPa; Poisson's ratio that varied from 0.1 to 0.49. The shear strength and body load parameters of the problem presented by Leshchinsky et al. (1985) are as follows: total cohesion of 0.116 kPa; friction angle of 15^o; pore-water pressure equal to zero; and unit weight of 1 kN/m^3.

Even though Leshchinsky et al. (1985) have used logarithmic spirals, a spherical

shape approximates the shape of the original slip surface fairly well. Figure 2a presents the slip surface adopted herein. The radius and center were adjusted in order to match the original slip surfaces. Subtle differences in the position of the slip surfaces adopted by Hungr et al. (1989) and Stianson (2006) were matched.

Figure 2b presents the distribution of vertical stresses throughout the slope. Once again, the simple geometry and absence of external loads results in smooth contours for the distribution of stresses.

Table 2 presents the results obtained by the three previous researchers and those obtained in this study. The differences in factor of safety among the three previous researchers are due to differences in the method of analysis and, more importantly, differences in the position of the slip surfaces obtained. The factors of safety appear to be reasonably close when comparing those obtained by each author and the results presented herein. Poisson's ratio appears to have an effect on the factor of safety. Higher Poisson's ratios result in higher factors of safety.

CONCLUSIONS

A practical three-dimensional slope stability approach was presented, using simple finite element stress and seepage analyses. Benchmark problems were presented in order to verify the accuracy of the proposed method. Close agreement was observed when comparing the results obtained herein and those from in the literature. Higher values of Poisson's ratio resulted in higher values of factor of safety.

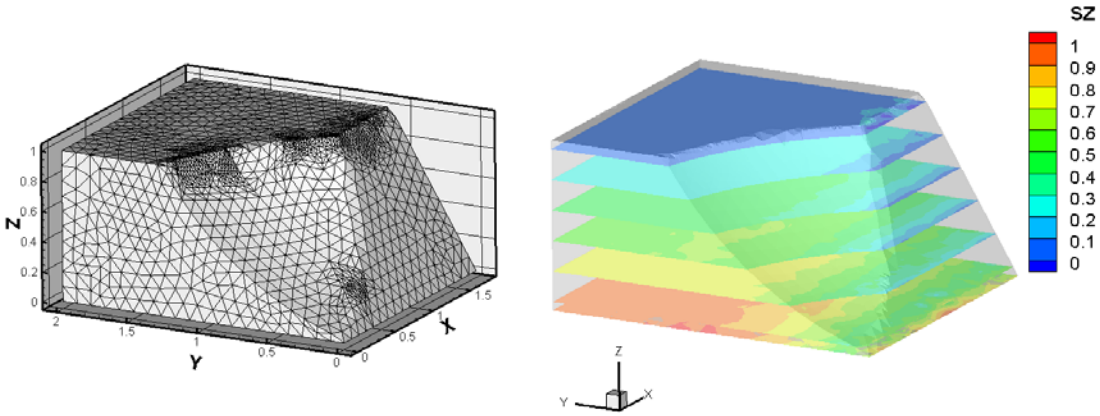

(a) (b)

FIG. 2. Benchmark problem 2: (a) geometry and slip surface shape matching that of Leshchinsky et al. (1985); and (b) distribution of vertical stresses.

Table 2. Benchmark problem 2: factors of safety obtained by other research and obtained in this study.

Reference	Fs 3-D	This study, Fs 3-D				
		μ = 0.1	μ = 0.2	μ = 0.3	μ = 0.4	μ = 0.49
Leshchinsky et al. (1985)	1.250	1.209	1.221	1.234	1.246	1,258
Hungr et al. (1989)	1.230	1.239	1.247	1.256	1.265	1,277
Stianson (2006)	1.410	1.354	1.368	1.382	1.395	1,408

ACKNOWLEDGMENTS

The authors would like to thank "Conselho Nacional de Desenvolvimento Científico e Tecnológico – CNPq, Brasil", for financial support and Jason Stianson for the discussions and for providing unpublished data from his PhD research.

REFERENCES

Baligh, M. M. and Azzouz, A. S. (1975). End effects on stability of cohesive slopes. ASCE J. of the Geotech. Engng. Div., 101 (11): 1105-1117.

Chen, J., Yin, J.-H., and Lee, C.F. (2001). Upper Bound Limit analysis of slope stability using rigid finite elements and nonlinear programming Can. Geotech. J., 40: 742-752.

Chen, Z. Y., Wang, X. G., Haberfield, C., Yin, J. H. and Wang, Y. J. (2001a). A three-dimensional slope stability analysis method using the upper bound theorem. Part I: Theory and methods. Int. J. Rock Mech. Mining Sci. 38: 369–378.

Chen, Z. Y., Wang, J., Wang, Y. J., Yin, J. H. and Haberfield, C. (2001b). A three-dimensional slope stability analysis method using the upper bound theorem. Part II: Numerical approaches, applications and extensions. Int. J. Rock Mech. Mining Sci. 38: 379-397.

Farzaneh, O. & Askari, F. (2003). Three-dimensional analysis of nonhomogeneous slopes. J. Geotech. Geoenviron. Engng ASCE, 129(2): 137-145.

Gens, A., Hutchison, J.N., and Cavounidis, S. (1988). Three-dimensional analysis of slopes in cohesive soils. Géotechnique, 38 (1): 1-23.

Hungr, O., Salgado, F.M. and Byrne, P.M. (1989). Evaluation of a three-Dimensional Method of Slope stability analysis. Can. Geotech. J. 26: 679-686.

Lam, L. and Fredlund, D.G (1993). A general limit equilibrium model for three-dimensional slope stability analysis, Can. Geotech. J. 30: 905-919.

Leshchinsky, D., Baker, R. and Silver, M. L. (1985). Three dimensional analysis of slope stability. Int. J. Numer. Anal. Methods Geomech., 9: 199–223.

Leshchinsky, D. and Baker, R. (1986). Three-dimensional slope stability: end effects. Soil and Foundations, 26 (4): 98-110.

Leshchinsky, D. and Huang, C. C. (1992). Generalized three-dimensional slope stability analysis. J. Geotech. Engng ASCE 118 (11): 1748–1764.

Lyamin, A. V. & Sloan, S. W. (2002a). Lower bound limit analysis using nonlinear programming. Int. J. Numer. Methods Engng, 55 (5): 573–611.

Lyamin, A. V. & Sloan, S. W. (2002b). Upper bound limit analysis using linear finite elements and non-linear programming. Int. J. Numer. Anal. Methods Geomech., 26: 181-216.

Michalowski, R. L. (1989). Three-dimensional analysis of locally loaded slopes. Geotechnique, 39 (1): 27–38.

PDE Solutions Inc. (2007). FlexPDE 5.0 - Reference Manual, Antioch, CA, USA.

SoilVision Systems Ltd. (2007). "SVOffice 2006 User's and Theory Guide." Saskatoon, SK, Canada.

Stianson, J. (2006). Personal communication.